Driver torque estimation in Electric Power Steering system using an H_∞/H_2 Proportional Integral Observer

Kazusa Yamamoto [1,2], Damien Koenig [1], Olivier Sename [1] and Pascal Moulaire [2]

Abstract— **This paper deals with the design of a Proportional Integral (PI) observer to estimate the driver torque in an Electric Power Steering (EPS) system. The PI observer is obtained by solving a multi-objective optimization problem: it should both be barely sensitive to road disturbances and sensor noise, and converge swiftly. The performance of the proposed observer is illustrated by simulation results using experimental data.**

I. INTRODUCTION

Currently, most of the vehicles uses Electric Power Steering (EPS) systems. Indeed, compared to hydraulic steering systems, EPS systems improve fuel efficiency (with a fuel economy up to 5%), quality of feedback to the driver and ease of integration in the vehicle.

In modern vehicles, steering systems help the driver turn the vehicle, improving both safety and comfort. In order to do so, an assistance torque is provided by an electric assistance motor, to reduce the amount of torque required from the driver to turn the wheels in the desired direction. The amount of supplied power is defined by the Electronic Control Unit (ECU) according to a motor torque control policy, containing an assistance rule depending on the vehicle speed and measurements from a torque sensor [1].

A. Problem statement

Reducing production costs (*e.g* by removing a sensor) and improving the performance of EPS control system is a challenge for EPS system suppliers in the automotive market. One of the main requirements in EPS systems is to determine the amount of assist torque to provide. This is usually done using a torque sensor to measure applied steering torque. However, failure of this sensor could lead to a sudden loss of steering assistance. For driving comfort and safety reasons, such an event should be avoided. Moreover, it may be noted that the output of the torque sensor is reliable while the driver torque is constant and the assist motor is not providing an additional torque [2],[3]. Developing a controller based on sensorless driver torque estimation may offer improvements in both production costs and performance by providing a better estimation of the actual value of the driver torque [3],[4].

[1] Kazusa Yamamoto, Damien Koenig, Olivier Sename are with GIPSA-Lab, Control system department, Université Grenoble-Alpes, 11 rue des Mathematiques, BP46, 38402 Saint Martin d'Heres Cedex, France (`kazusa.yamamoto,damien.koenig,olivier.sename`) `@gipsa-lab.grenoble-inp.fr`
[2] Kazusa Yamamoto and Pascal Moulaire are with JTEKT Europe, ZI du Broteau, BP1, 69540 Irigny, France (`kazusa.yamamoto,pascal.moulaire`)`@jtekt-eu.com`

B. State of the art

Several studies have already been carried out on driver torque estimation in EPS systems. Marouf et al. proposed in [2], [4], [5], a Sliding Mode Observer (SMO) to estimate both the driver torque and the road reaction force in an EPS system. However, it does not satisfy the observer matching condition, since additional inputs for the observer are generated using High Order Sliding Mode Differentiator (HOSMD). The SMO is based on a simplified EPS state-space representation and uses as inputs the steering wheel angle and the absolute angular position of the motor ("motor angle" in the remainder of this paper). [2] studies a resolverless EPS system, in which motor angle is computed using HOSMD on the measured motor current, whereas in [4], [5] the two angles are measured. In [6], an observer computing the driver and load torque is designed by pole placement. In this case, the measured inputs of the observer are the torque sensor signal and the steering column speed. Another estimator is introduced in [3] and [7] using the torque sensor signal and the assist motor input current. The estimator is deduced from the EPS transfer function model. However, in order to get a stable transfer function in the specified frequency range, approximations have been made in computing the estimator. In [8] an indirect estimation is used to compute the driver torque, since it is deduced from estimation of the road reaction torque and the motor shaft torque. These torques are computed using a model of the vehicle dynamics and a Direct Current (DC) motor model. In [9] a Kalman filter is implemented to estimate all the states of a dual-pinion EPS system. Motor angle and voltage are the required measurements.

These previous studies show that driver torque estimation is still an open issue. The challenge is to avoid the need of a torque sensor to estimate the driver torque. Moreover the estimation algorithm should be implementable under some software/hardware constraints *e.g* ECU storage space. Moreover, the implementation of the observer on a mass-produced vehicle requires developing new safety concepts with respect to embedded complexity, which is made easier by using a linear observer.

C. Contribution

The main contribution of this paper is the application-oriented design of a PI observer to estimate the driver torque on an EPS system. The steering wheel angle and the assist motor angle are required inputs measurements for the PI observer. Then, the observer gains are chosen to get a fast

estimation and to minimize the effects of road disturbances (resp. sensor noise) on the driver torque estimation error, in an H_∞ framework (resp. H_2 framework).

This paper is organized as follows. Section II presents the EPS model limited to its mechanical relations. Section III describes the multi-objectives design of the PI observer, and section IV shows synthetic results based on numerical simulation. Then, performance of the PI observer are illustrated by simulation results using experimental data in section V. Finally, section VI leads to the conclusions and future works.

II. EPS SYSTEM MODEL

Mechanical model of EPS

The EPS system can be decomposed into four main parts: the steering wheel, the assist motor, the pinion and the rack. The pinion type EPS (P-EPS) simplified mechanical model structure is illustrated in Figure 1 similarly as in [10].
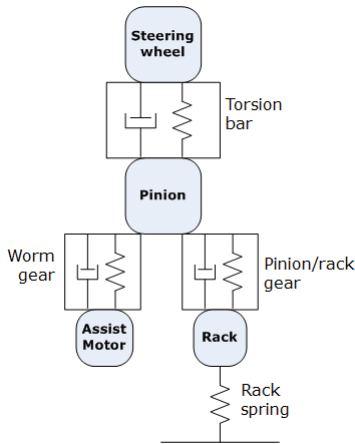

Fig. 1.   P-EPS mechanical model

Applying Newton's laws of motion and neglecting dry friction, the P-EPS model is governed by the equations:

$$J_c\ddot{\theta}_c = \tau_d - \Big(D_{tb}(\dot{\theta}_c - \dot{\theta}_p) + K_{tb}(\theta_c - \theta_p)\Big) - B_c\dot{\theta}_c \quad (1)$$

$$J_m\ddot{\theta}_m = \tau_m - \Big(D_g(\dot{\theta}_m - G\dot{\theta}_p) + K_g(\theta_m - G\theta_p)\Big) - B_m\dot{\theta}_m \quad (2)$$

$$\begin{aligned} J_p\ddot{\theta}_p = {}& \Big(D_{tb}(\dot{\theta}_c - \dot{\theta}_p) + K_{tb}(\theta_c - \theta_p)\Big) \\ & + G\Big(D_g(\dot{\theta}_m - G\dot{\theta}_p) + K_g(\theta_m - G\theta_p)\Big) \\ & - R_p\Big(D_{pr}(R_p\dot{\theta}_p - \dot{X}_r) + K_{pr}(R_p\theta_p - X_r)\Big) \end{aligned} \quad (3)$$

$$\begin{aligned} J_r\ddot{X}_r = {}& \tau_{road} + \Big(D_{pr}(R_p\dot{\theta}_p - \dot{X}_r) + K_{pr}(R_p\theta_p - X_r)\Big) \\ & - \Big(D_r\dot{X}_r + K_rX_r\Big) - B_r\dot{X}_r \end{aligned} \quad (4)$$

where the variables are θ_c the steering wheel angle (rad), θ_m the motor angle (rad), θ_p the pinion angle (rad), X_r the rack position (m) and the mechanical parameters are described in Table I.

Hence the state-space representation of the P-EPS system

Notation	Description	Unit
J_c	Steering column inertia	$kg.m^2$
B_c	Steering column viscous friction	$N.m/(rad/s)$
K_{tb}	Torsion bar stiffness	$N.m/rad$
D_{tb}	Torsion bar damping	$N.m/(rad/s)$
J_p	Pinion/gear inertia	$kg.m^2$
K_{pr}	Pinion/rack stiffness	N/m
D_{pr}	Pinion/rack damping	$N/(m/s)$
R_p	Pinion/rack reducer	m/rad
J_r	Rack and tie rods mass	kg
B_r	Rack viscous friction	$N/(m/s)$
K_r	Rack stiffness	N/m
D_r	Rack damping	$N/(m/s)$
G	Worm/gear reduction ratio	$-$
J_m	Motor inertia	$kg.m^2$
B_m	Motor viscous friction	$N.m/(rad/s)$
K_g	Worm/gear stiffness	$N.m/rad$
D_g	Worm/gear damping	$N.m/(rad/s)$

TABLE I

EPS SYSTEM MECHANICAL PARAMETERS

is the following:

$$\begin{cases} \dot{x} = Ax + Bu + Ed + Ww \\ y = Cx + Nn \end{cases} \quad (5)$$

with $x = \begin{pmatrix} \dot{\theta}_c & \dot{\theta}_m & \dot{\theta}_p & \dot{X}_r & \theta_c & \theta_m & \theta_p & X_r \end{pmatrix}^T \in \mathbb{R}^{n_x}$ are the internal states, $d \in \mathbb{R}$ is the driver torque to be estimated, $w \in \mathbb{R}$ the road reaction torque is the unknown input, and $u \in \mathbb{R}$ the assist motor torque is the control signal. The available measurements are $y = \begin{pmatrix} \theta_c & \theta_m \end{pmatrix}^T \in \mathbb{R}^{n_y}$ which are affected by white gaussian noise $n \in \mathbb{R}$. Moreover N is the weighting matrix associated to n in the form $N = \beta I$ with $\beta \in \mathbb{R}^+$.

In this paper the model identification and validation are not detailed. However, the given model was validated upon experimental data on the relevant frequency domain. Figure 2 shows the typical experimental and simulated frequency responses (computed as described in [11]) used to validate the model. In this case, the signal is applied as the motor torque input (control signal). Using a sinus of amplitude $10N.m$ with frequency from 0.1 to $60Hz$, the obtained transfer function from control signal to motor angle $T_{\theta_m u}$ is shown below in Figure 2.
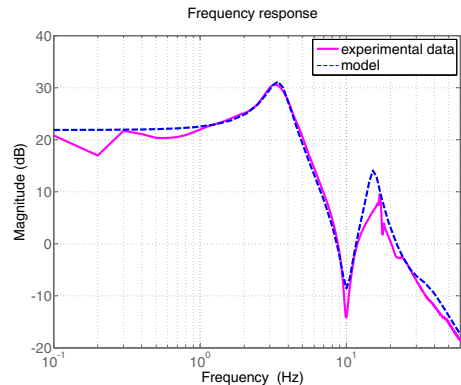

Fig. 2.   Frequency domain model validation of $T_{\theta_m u}$

III. PI OBSERVER DESIGN

The main objective is to estimate the unmeasured driver torque input d, considering the unknown input w as a disturbance. Such a problem is similar to the unknown input observer design problem as described in [12], [13]. However, the system (5) does not fulfill the exact disturbance decoupling condition. Therefore, a H_∞/H_2 PI observer is proposed to minimize the effect of sensor noise and road disturbances while providing a fast convergence of the estimation. Moreover, it should be ensured that driver torque acts in low frequency, since the PI observer dynamic allows to estimate constant and slowly time varying input.

In order to specify the frequency range for disturbance attenuation, a weighting function $W_f(s)$ is introduced as:

$$w = W_f(s)\bar{w} \Leftrightarrow \begin{cases} \dot{x}_w = A_w x_w + B_w \bar{w} \\ w = C_w x_w + D_w \bar{w} \end{cases} \quad (6)$$

Indeed, the road reaction force can reach up to $10kN$ for parking manoeuvres. This means even an attenuation of $-60dB$ implies an error on the estimation up to $10N.m$, whereas the driver torque doesn't exceed $30N.m$. The weighting function is therefore used to specify a frequency domain where the disturbance w should be attenuated.

The augmented representation combining (5) and (6) is:

$$\begin{cases} \dot{x}_a = A_a x_a + B_a u + E_a d + W_a \bar{w} \\ y = C_a x_a + N n \end{cases} \quad (7)$$

where $x_a = \begin{pmatrix} x^T & x_w^T \end{pmatrix}^T$ are the augmented states and the associated matrices are $A_a = \begin{pmatrix} A & WC_w \\ 0 & A_w \end{pmatrix}$, $W_a = \begin{pmatrix} WD_w \\ B_w \end{pmatrix}$, $E_a = \begin{pmatrix} E \\ 0 \end{pmatrix}$, $B_a = \begin{pmatrix} B \\ 0 \end{pmatrix}$, $C_a = \begin{pmatrix} C & 0 \end{pmatrix}$.

The PI observer for the augmented representation (7) is written as follows :

$$\begin{cases} \dot{\hat{x}}_a = A_a \hat{x}_a + E_a \hat{d} + L_p(y - C_a \hat{x}_a) + B_a u \\ \dot{\hat{d}} = L_i(y - C_a \hat{x}_a) \end{cases} \quad (8)$$

The condition for the existence of the observer is that the pair $\left(\begin{bmatrix} A_a & E_a \end{bmatrix}, \begin{bmatrix} C_a & 0 \end{bmatrix} \right)$ is detectable *i.e*

$$rank \begin{bmatrix} pI - A_a & -E_a \\ 0 & pI \\ C & 0 \end{bmatrix} = n_{x_a} + n_d \quad (9)$$

$\forall p \in \mathbb{C}$ such that $Re(p) \geq 0$. Here $n_{x_a} = n_x + n_w$ and n_d denote the number of states x_a in (7) and $n_d = 1$ refers to the state d of the driver torque.

Defining the extended state $\begin{pmatrix} x_a^T & d^T \end{pmatrix}^T$ and the estimation error $e_{ad} = \begin{pmatrix} (x_a - \hat{x}_a)^T & (d - \hat{d})^T \end{pmatrix}^T$ and assuming $\dot{d} \approx 0$ (however this might be a restrictive hypothesis for evasive manoeuvres that imply fast driver dynamic), the dynamic of the estimation error deduced from (7) and (8) is:

$$\begin{cases} \dot{e}_{ad} = (A_{ad} - L_a C_{ad})e_{ad} + W_{ad}w + L_a N n \\ \tilde{z} = D_{ad} e_{ad} \end{cases} \quad (10)$$

where $L_a = \begin{pmatrix} L_p & L_i \end{pmatrix}^T$ is the observer gain to be deter-

mined, $\tilde{z} = d - \hat{d}$ is the observer output and the associated matrices are $A_{ad} = \begin{pmatrix} A_a & E_a \\ 0 & 0 \end{pmatrix}$, $W_{ad} = \begin{pmatrix} W_a \\ 0 \end{pmatrix}$, $C_{ad} = \begin{pmatrix} C_a & 0 \end{pmatrix}$, $D_{ad} = \begin{pmatrix} 0 & 1 \end{pmatrix}$. From (10), $A_{ad} - L_a C_{ad}$ is Hurwitz if and only if the pair (A_{ad}, C_{ad}) is detectable, or equivalently:

$$rank \begin{bmatrix} pI - A & -WC_w & -E \\ 0 & pI - A_w & 0 \\ 0 & 0 & pI \\ C & 0 & 0 \end{bmatrix} = n_x + n_w + n_d \quad (11)$$

$\forall p \in \mathbb{C}$ such that $Re(p) \geq 0$. Here n_x and n_w denotes the number of states x in (5) and x_w in (6). Since a stable weighting function is chosen for (6), (11) comes to:

$$rank \begin{bmatrix} pI - A & -E \\ 0 & pI \\ C & 0 \end{bmatrix} = n_x + n_d \quad (12)$$

for all p such that $Re(p) \geq 0$. For (5) the condition (12) is satisfied thus the observer described in (8) exists.

Figure 3 shows the augmented representation and the observer. Plant inputs are the unknown input w specified on a frequency range, the driver torque d to estimate and the control signal u. The PI observer inputs are the control signal u, the measured plant output y affected by sensor noise n. Its output is the estimated driver torque $\hat{d}$.
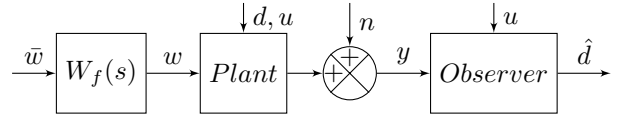

Fig. 3. Block diagram of the augmented system and observer

As explained below, the first design objective is to ensure the performances of the estimation through the specifications of the observer poles. On the other hand, even if the observer estimates all the internal states $\hat{x}_a$, the performance objective will focus only on the minimization of the driver torque estimation error $d - \hat{d}$ which explains the choice of $\tilde{z}$. Then, the design of the observer aims at minimizing the effect of road disturbances (resp. sensor noise) subject to H_∞-norm (resp. H_2-norm) on the driver torque estimation error. This needs to handle the sensitivity functions deduced from (10) :

$$T_{\tilde{z}\bar{w}} = D_{ad} \left(sI - (A_{ad} - L_a C_{ad}) \right)^{-1} W_{ad} \quad (13)$$

$$T_{\tilde{z}n} = D_{ad} \left(sI - (A_{ad} - L_a C_{ad}) \right)^{-1} L_a N \quad (14)$$

A. Pole placement

As the observer dynamic response is defined by the eigenvalues of $(A_{ad} - L_a C_{ad})$, setting an upper bound λ_{min} on the real part of the observer poles ensures a fast convergence of the estimate. Indeed, the other poles are in that case greater than λ_{min}. Such a constraint is formulated as the following Linear Matrix Inequality (LMI) condition developed in [14],[15]:

$$A_{ad}^T P + P A_{ad} - C_{ad}^T Y - Y C_{ad} + 2\lambda_{min} P < 0 \quad (15)$$

where $Y = PL_a$ with P a positive definite matrix, the observer gain L_a is deduced as $L_a = P^{-1}Y$ after solving the LMI equations. Using L_a as in (15) for the observer gain ensures that all the poles are in the left-half plane region $Re(\lambda) < \lambda_{min}$.

B. H_∞ performance

As stated in the beginning of section III, the road reaction disturbance w should be highly attenuated. In practice, it is sufficient to minimize the disturbance effects on the frequency domain of interest for the considered application. The weighting function described in (6) is a filter, where the design parameters are the minimal bandwith ω_b, the steady state error k_1 and the maximum of the sensibility function K_1. In practice, the road disturbance has to be rejected in low frequencies (up to $30Hz$), as it is the range of frequencies for driver's torque inputs. The minimization of the disturbances $\bar{w}$ on the driver torque estimation error $\tilde{z}$ is handled using H_∞-norm, determined by bounding the transfer function $\tilde{z}$ to $\bar{w}$. The problem formulation is given as: minimize γ_∞ such that $||T_{\tilde{z}\bar{w}}||_\infty \leq \gamma_\infty^2$. Thus the LMI below is satisified:

$$\begin{pmatrix} A_{ad}^T P + P A_{ad} - C_{ad}^T Y - Y C_{ad} + D_{ad}^T D_{ad} & P W_{ad} \\ * & -\gamma_\infty^2 \end{pmatrix} < 0 \tag{16}$$

let $*$ denotes the symmetric element.

C. H_2 performance

The minimization of the effect of sensor noise n on the driver torque estimation error $\tilde{z}$ is handled using the generalized H_2-norm, of the transfer function from $\tilde{z}$ to n (sse [16]). The problem formulation is given as: minimize γ_2 such that $||T_{\tilde{z}n}||_\infty \leq \gamma_2^2$. Thus the LMIs below are satisfied:

$$\begin{pmatrix} A_{ad}^T P + P A_{ad} - C_{ad}^T Y - Y C_{ad} & -YN \\ * & -I \end{pmatrix} < 0$$

$$\begin{pmatrix} P & D_{ad}^T \\ * & \gamma_2^2 \end{pmatrix} > 0 \tag{17}$$

It is worth noting that, as in subsection B, a weighting function could be introduced to specify the frequency range on which sensor noise should be attenuated. Besides, sensor noise itself is a high frequency signal.

D. Design procedure in the H_∞/H_2 framework

Proposition 1: Consider the system model (5) under the assumption $\dot{d} = 0$ and the PI observer described in (8).

If there exists $P = P^T > 0$ and Y satisfying: $min\ \alpha\gamma_\infty + (1-\alpha)\gamma_2$ with $\alpha \in [0;1]$ with positive scalars γ_∞, γ_2 subject to the LMIs (15)–(17). Then, the observer (8) is an H_∞/H_2 PI observer with the gain $L_a = P^{-1}Y$.

Note that a common Lyapunov matrix P has been used to ensure convexity to the multi-objective problem [15].

IV. DESIGN ANALYSIS

In this part, numerical synthesis results computed from the design described in Section III are presented. First, the results obatined with an observer satisfying the hypothesis of *Proposition* 1 are shown. Then, a comparison is made between design performances of H_∞, H_2 and H_∞/H_2.

Finding L_a such as described in *Proposition* 1, the following results are deduced: taking $\alpha = 0.5$, the attenuation level is given by $\gamma_\infty = 0.2365$ and $\gamma_2 = 0.645$. Moreover, Figure 4 shows the region of the resulting pole placement.
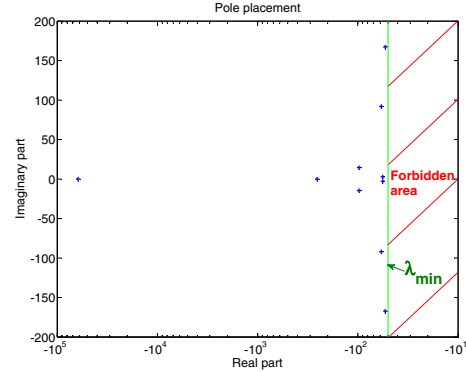

Fig. 4. Observer's poles

To see the efficiency of H_∞/H_2, a comparison with H_∞ and H_2 performance has been carried out. From (10) the effective attenuation subject to minimization of H_∞-norm is shown by the Bode diagram of the transfer function from the disturbance w to the driver torque estimation error $\tilde{z}$:

$$|T_{\tilde{z}w}| < |W_f^{-1}|\gamma_\infty^2 \tag{18}$$

Figure 5 shows the resulting attenuation of the disturbance on the estimation error subject to the minimization problems H_∞, H_2 and H_∞/H_2. Note that all methods meet the requirements (18).
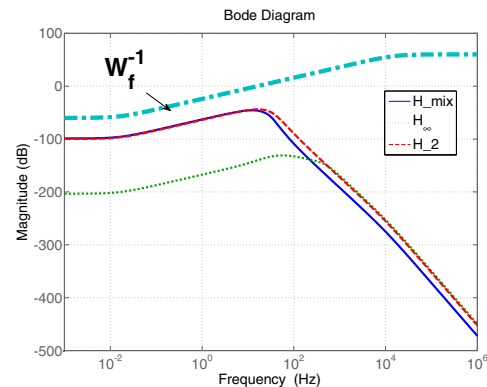

Fig. 5. Comparison between H_∞, H_2 and H_∞/H_2 design performance on $T_{\tilde{z}w}$

Figure 6 shows the resulting attenuation of the sensor noise on the estimation error subject to the minimization problems H_∞, H_2 and H_∞/H_2. The left side illustrates the attenuation of the driver torque estimation error $\tilde{z}$ depending on the sensor noise on the steering wheel angle $y_1 = \theta_c + \beta n$ and the right one depending on the sensor noise on the motor angle $y_2 = \theta_m + \beta n$.
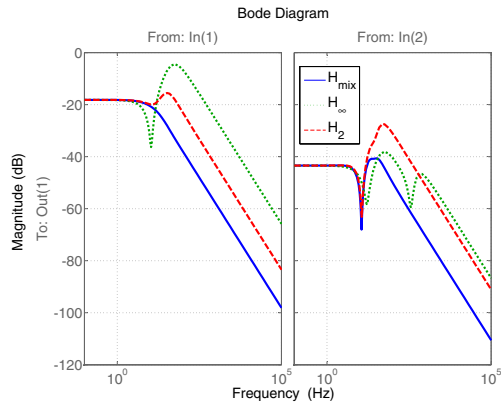
Bode Diagram

Fig. 6. Comparison between H_∞, H_2 and H_∞/H_2 design performance on $T_{\tilde{z}n}$

Figure 7 shows the bandwidth of the observer subject to the result of the minimization problem H_∞, H_2 and H_∞/H_2. The transfer function $T_{\hat{d}d}$ is deduced from (5) and (8):

$$T_{\hat{d}d} = D_{ad}(sI-(A_{ad}-L_aC_{ad}))^{-1}L_a.C(sI-A)^{-1}E \quad (19)$$

Bode Diagram
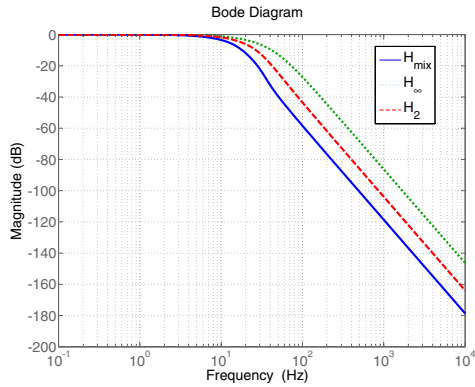

Fig. 7. Comparison between H_∞, H_2 and H_∞/H_2 design performance on $T_{\hat{d}d}$

In Table II the norms of $||T_{\tilde{z}w}||_\infty$ and $||T_{\tilde{z}n}||_2$ obtained from the resulting observers following the three minimization problems H_∞, H_2 and H_∞/H_2 are shown.

	H_2	H_∞	H_∞/H_2
$\|T_{\tilde{z}w}\|_\infty$	6.5382E-3	2.8892E-7	4.5015E-3
$\|T_{\tilde{z}\theta_c}\|_2$	1.974	9.6728	0.6459
$\|T_{\tilde{z}\theta_m}\|_2$	0.5917	0.3028	7.2380E-2

TABLE II

COMPUTED NORM OF $T_{\tilde{z}n}$ AND $T_{\tilde{z}n}$ SUBJECT TO STRATEGIES H_∞, H_2 AND H_∞/H_2

Hence the mixed H_∞/H_2 problem is the best compromise between attenuation of disturbance and sensor noise.

V. RESULTS

In this part the experimental results obtained with the designed observer described in Section V are shown.

The PI observer has been tested using experimental data gathered on a development vehicle equipped with a P-EPS system. Besides the usual motor resolver and torque sensor used in P-EPS system, a steering sensor and driver torque sensor have been added to the vehicle. Figure 8 illustrates the simulation block diagram implemented on Matlab/Simulink.

Fig. 8. Block diagram of the implemented observer

In the following simulation results, the measured steering wheel angle, motor angle and driver torque are sampled every $10ms$; the implemented observer is also discretized at the same rate. From figure 9, the frequency response of the continuous and discretized observer are very close, ensuring a good implementation.
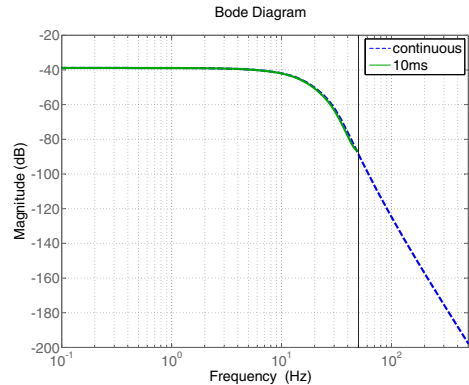
Bode Diagram

Fig. 9. Comparison between continuous PI observer and discretized PI observer at 10ms

The experimental data comes from a rolling condition without assist torque ($u = 0N.m$) on a test track.

A. Test 1: rolling on the track

Figure 10 shows the comparison between the measured driver torque and the estimated torque, when the driver goes around the track. Therefore, vehicle speed and direction are time-varying.

B. Test 2: sinusoidal driving

Figure 11 shows the comparison between the measured driver torque and the estimated torque, in a particular driving condition. It involves following an "8" shaped pattern on the track at a constant speed of $20kph$. This test allows to simulate a sinusoidal driver torque. The root mean squared

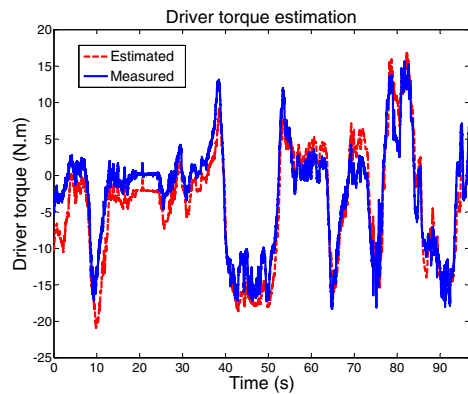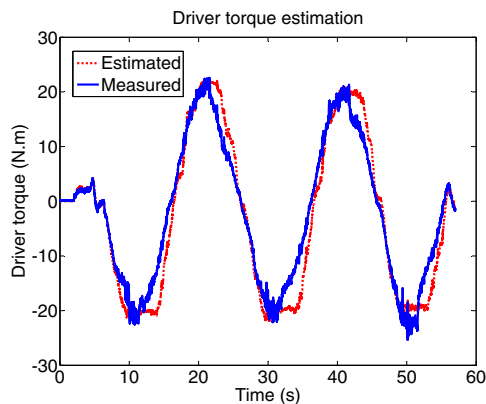Fig. 10. Driver torque estimation - Test 1

Fig. 11. Driver torque estimation - Test 2

error (RMSE) is calculated as:

$$RMSE = \sqrt{\frac{\sum_{i=1}^{m}(d_{measured}(i) - \hat{d}(i))^2}{m}} \qquad (20)$$

where m is the number of data points. The resulting RMSE for test 1 is $3.21N.m$ and for test 2 is $3.63N.m$. Moreover the normalized RMSE on the whole range is 7% for test 1 and 8.32% for test 2.

According to the above simulation results, it can be seen that the observer has a good dynamic transition and an acceptable convergence to the estimated value. Thus performance of the PI observer are validated on experimental data.

VI. CONCLUSIONS

In this paper, an estimation of a P-EPS system driver torque has been proposed using a PI observer. The observer has been designed subject to pole placement and H_∞/H_2 minimization objectives. Then, the performance of the resulting observer has been evaluated by simulation using experimental measurements.

An industrial interest could be, at first, to develop a limp-home operation mode. This means that even if a failure occurs on the torque sensor, an assistance torque (computed from the PI observer) could be provided to the driver. Future works will concentrate on further improvements to the ob-

server performance. The road reaction force, *e.g* represented with Lugre model, should be included in the EPS model (5).

Even though the observer can still be improved, it is satisfactory enough to be tested on an actual vehicle using an existing control scheme [17]. Unlike previous field testings, the observer will be evaluated in the presence of an assist torque ($u \neq 0$). Depending on the results, a motor model might be added in (5) or a new controller based on the PI observer might be designed to get a more efficient observer. Furthermore a robustness analysis of the closed-loop system including the observer and controller could be carried out.

REFERENCES

[1] V.N. Sulakhe,M.A. Ghodeswar, M.D. Gite, Electric Power Assisted Steering, Journal of Engineering Research and Applications, vol.3, pp. 661-666, 2013

[2] A. Marouf, M. Djemaï, C. Sentouh and P. Pudlo, Sensorless control of Electric Power Assisted Steering system, 20th Mediterr. Conf. Control Autom., Barcelona (Spain) pp. 909–914, 2012

[3] R.C. Chabaan, Torque Estimation in Electrical Power Steering Systems, IEEE Veh. Power Propuls. Conf., Dearborn (USA), pp. 790–797, 2009

[4] A. Marouf, M. Djemaï, C. Sentouh and P. Pudlo, A new Control Strategy of an Electric Power Assisted Steering system, IEEE Trans. Veh. Technol., vol. 61, pp. 3574–3589, 2012

[5] A. Marouf, M. Djemaï, C. Sentouh and P. Pudlo, Driver torque and road reaction force estimation of an electric power assisted steering using sliding mode observer with unknown inputs, IEEE Conf. Intell. Transp. Syst., Funchal (Portugal), pp. 354–359, 2010

[6] J. Tordesillas Illán, V. Ciarla and C. Canudas de Wit, Oscillation annealing and driver/tire load torque estimation in Electric Power Steering systems, IEEE Int. Conf. Control Appl., Denver (USA), pp. 1100–1105, 2011

[7] R.C. Chabaan and L.Y Wang, Control of Electrical Power Assist Systems : H_∞ Design Torque Estimation and Structural Stability, JSAE Review, vol. 22, pp. 435–444, 2001

[8] S. Cholakkal and X. Chen, Fault tolerant control of electric power steering using robust filter-simulation study, IEEE Veh. Power Propuls. Conf., Dearborn (USA), pp. 1244–1249, 2009

[9] M. Parmar and J.Y. Hung, Modeling and sensorless optimal controller design for an electric power assist steering system, IEEE 28th Annu. Conf. Ind. Electron. Soc., vol.3, pp. 1784–1789, 2002

[10] A. Badawy, J. Zuraski, F. Bolourchi A.and Chandy, Modeling and Analysis of an Electric Power Steering System, SAE Tech. Paper, 1999

[11] C. Poussot-Vassal, O. Sename, L. Dugard, P. Gáspár, Z. Szabó and J.Bokor, A new semi-active suspension control strategy through LPV technique, Control Enginnering Practice, vol. 16, pp 1519–1534, 2008

[12] S. Hui and S.H. Zak, Observer Design for Systems With Unknown Inputs, Int. J. Appl. Math. Comput. Sci., vol. 15, pp. 431–446, 2005

[13] Y. Xiong and M. Saif, Unknown disturbance inputs estimation based on a state functional observer design, Automatica, vol. 39, pp. 1389–1398, 2003

[14] L. Dugard, O. Sename, S. Aubouet, and B. Talon, Full vertical car observer design methodology for suspension control applications, Elsevier Control Eng. Pract., vol. 20, pp. 832–845, 2012

[15] M. Chilali and P. Gahinet, H_∞ Design with pole placement constraints: an LMI Approach, IEEE Transactions on Automatic Control, vol. 41, pp. 358–367, 1996

[16] C. Scherer and S. Weiland, Linear matrix inequalities in control, Lecture notes, 2000

[17] A. Michelis, P. Pilaz, P. Moulaire and S. Gaudin, Method for determining a torque set value for a steering wheel for a power steering system of a motor vehicle, US Patent 8 924 038, 2014